Measurement 265 (2026) 120358



Contents lists available at ScienceDirect

Measurement

journal homepage: www.elsevier.com/locate/measurement



Role of water service lines in the propagation of user-induced transients: Laboratory investigation on a highly instrumented, full-scale replica

Valentina Marsili [a,*], Debora Falocci [b], Caterina Capponi [b], Filippo Mazzoni [a], Stefano Alvisi [a], Bruno Brunone [b], Silvia Meniconi [b]

[a] Department of Engineering, University of Ferrara, Via Saragat 1, 44122 Ferrara, Italy
[b] Department of Civil and Environmental Engineering, University of Perugia, Via Duranti 93, 06125 Perugia, Italy

ARTICLE INFO

Keywords:
Water distribution network
High-frequency pressure monitoring
Pressure transients
Laboratory experiments
Pipe fatigue
Water service line
Plumbing system
Water hammer

ABSTRACT

Water service lines (SLs) are the hydraulic interface between the water distribution network and household plumbing systems (PSs). However, their vulnerability to rapid pressure transients caused by everyday household water use is still poorly understood due to the scarcity of detailed experimental investigation. Therefore, a highly instrumented full-scale laboratory replica of a complete "minor system", consisting of a SL and a PS, was developed to: (*i*) comprehensively measure user-induced transients under fully controlled conditions, and (*ii*) investigate how SL characteristics govern those transients. The facility incorporates interchangeable SLs of various diameters and materials commonly used in practice, as well as a branched PS made up of pipes representative of modern residential installations. During a series of tests, flowrate and high-frequency pressure data were collected at several locations of the facility to accurately characterize the complex pressure wave dynamics. Step changes in demand were produced by a custom-built manoeuvring apparatus featuring fast-acting solenoid valves installed at four typical domestic outlets, ensuring repeatable test conditions. The analysis of high-frequency data revealed that closures generated pressure variations of up to 200 m within the plumbing system and 50 m within the SL; however, only a few meters were transmitted to the main network. Peak and cumulative hoop stresses were greatest for metallic and small-diameter SLs, and lowest for oversized and plastic SLs that promoted wave attenuation. The terminal branches of the PS experienced the greatest pressure variations, indicating them to be critical sections. The findings of the study clarify the mechanisms that contribute to the high failure rate of minor elements and provide quantitative guidance in the selection of the appropriate diameter and material during replacement operations. They also emphasize the importance of transient mitigation strategies for both utilities and users.

1. Introduction

Water Distribution Networks (WDNs) are crucial infrastructures aimed at delivering drinking water to the final user [1]. These systems consist of pipelines, typically organized in looped configurations, where storage facilities, pumps, and other hydraulic devices are installed to regulate the flow and pressure regime in the system. In WDNs, water is conveyed to the final user via service lines (SLs), which are small-diameter pipes that connect the main network to individual plumbing systems (PSs).

Despite being minor elements, SLs and private PSs play a crucial role in providing water of sufficient quality and pressure to the user. On the one hand, SLs are typically the last element managed by the water utility along with the water meter (i.e., the instrument that measures the volume of water supplied to users for billing purposes). On the other hand, the PS delivers water to each domestic device within the house and belongs to the private user. For technical and economical reasons, PSs are generally branched systems featuring small-diameter pipes. For residential users under continuous (24/7) pressurization, the SL supplies the PS in response to user demand, generating water-consumption events with defined intensity, duration, and frequency [2]. Alternatively, storage elements can be installed between the SL and the user's PS in case of non-residential users, e.g. manufacturing activities requiring water storage for multiple reasons (for instance, to face the interruption of water service for at least some hours in an emergency scenario), or when water is supplied intermittently [3–5].

* Corresponding author.
E-mail address: valentina.marsili@unife.it (V. Marsili).

https://doi.org/10.1016/j.measurement.2026.120358
Received 23 September 2025; Received in revised form 17 December 2025; Accepted 6 January 2026
Available online 7 January 2026
0263-2241/© 2026 The Authors. Published by Elsevier Ltd. This is an open access article under the CC BY-NC-ND license (http://creativecommons.org/licenses/by-nc-nd/4.0/).

The integrity of pipe systems, from the WDNs to PSs, is a fundamental requirement to ensure that safe water is efficiently delivered to the final users [6]. However, many practical issues undermine the reliability and resilience of WDNs [7]. One of the main weaknesses of pipe systems is represented by water losses, which pose challenges to water utilities and engineers [8–11]. Not only WDNs, but also minor elements such as SLs and PSs can be affected by leaks [12,13]. For many systems, losses on small-diameter pipes and the related fittings and connections represent the greatest number of leaks encountered in water supply operations – especially in systems where SL density is high [14,15]– with a tendency of SL failure rate to increase during the summer period [16]. In addition, it emerged that SLs are subjected to leaks that commonly go undetected for long periods with a consequent large wastage of drinking water [14]. A failed SL may also result in water quality problems due to the intrusion of untreated or contaminated water [17], posing a health concern in addition to water and energy waste [18]. Despite this, very limited information is available on leakage in PSs, an aspect which is only partially investigated by studies that exploit water consumption data from smart metering systems. In greater detail, these studies revealed that PSs are affected by leakage, with reported magnitude up to 100 L/person/day [2,19]. As expected, PS leakage is mainly due to pipe breaks or leaking valves and, thus, the related flowrate profiles are nearly constant throughout the day [20,21]. Although many factors can lead to the failure of SLs and PSs [22], recent studies show that pressure variations induced by user's activity through the activation of domestic devices might have a key role in increasing the vulnerability of these elements [23–25].

Pipe failures in WDNs stem from a complex interplay of environmental (e.g. soil corrosion, ground movement, frost-thaw cycles), intrinsic (e.g. pipe defects, careless installation, joint defects), and operational factors (e.g. internal pressure and external loadings) [26]. Among the operational factors, water pressure within WDNs emerges as a critical variable. In this regard, metrics adopted to describe the stress related to pressure in the pipe traditionally focus on static pressure measurements or daily average values, not accounting for the full range of pressure variation to which the pipe is subjected over a given time window. However, many examples in the literature revealed that pressure fluctuations which develop over a very short time frame are frequently observable in WDNs even under ordinary operational conditions [27–31]. These pressure transients are generated in WDNs by the operation of pumps and valves [28,32]. Recently, there has been evidence that users' activity [31,33–35] can also result in the generation of very frequent pressure waves.

The advent of new monitoring technologies – able to capture pressure changes during the transients by means of high-resolution (i.e., 10^{-1}-10^{1} kHz) measurements coupled with adequate acquisition systems – revealed that pressure fluctuations in WDNs are much more frequent than traditionally assumed [30,36,37]. This increased the interest in the research topic and prompted the measurement of these phenomena in both field and laboratory environments. Nevertheless, these fluctuating pressures can have a detrimental effect on WDN components (i.e. pipes, joints), potentially leading to fatigue in pipes as cyclic loadings [38,39] and highlighting the need for reduction and mitigation of these phenomena [40]; in extreme cases, a significant pressure change can also result in immediate damage, such as pipe burst or collapse, vibrations, and cavitation [41].

The interplay of mean pressure and pressure dynamics significantly contributes to the accumulation of long-term stress, material fatigue, and potential failures in WDNs. In greater detail, an increase in mean pressure can exacerbate the negative influence of pressure cycles, contributing to long-term fatigue, while factors such as manufacturing defects, pipe age and corrosion also play a role [42,43]. Overall, research findings indicate that minimizing pressure fluctuations is more beneficial than simply lowering mean pressure to mitigate fatigue, suggesting a combined approach to enhance pipe longevity and reduce failure rates [43]. It is straightforward that the correct characterization of factors contributing to pipe failure can foster the development of approaches to accurately forecast break rates [44], thus aiding utility companies in prioritizing pipe replacements and planning future investments [45]. However, despite the research achievements brought to date, wide margins remain to investigate the impact of water pressure on pipe breaks.

In this context, a new research branch is focusing on the characterization (i.e., measurement and interpretation) of pressure transients induced by users' activity, which are generated at a specific location in the users' PS and reach the WDN only after passing through and stressing the SL [23]. Despite this, only a few studies in the literature have explored the dynamic behaviour of SLs and PSs, almost exclusively through experimental approaches. Crucially, approaching the problem through modelling in non-elementary pipe systems remains challenging. When numerical attempts are made, capturing the macroscopic wave behaviour across the overall system is prioritized by adopting 1D modelling (e.g., Method of Characteristics). Conversely, modelling approaches aimed at reaching high level of detail, such as Computational Fluid Dynamics (CFD), while being a powerful tool for the optimal design of single hydraulic elements (e.g., [46]) or the analysis of the transient response of individual pipes (e.g., [47]), are impractical for application to complex pipe systems. In addition, the accurate prediction of system response ultimately relies on the rigorous validation of any hydraulic model through reliable experimental data.

A pioneer study by Lee et al. [48] explored the pressure range that affects a DN20 copper SL and the supplied PS (with a total length of about 50 m) by means of a simplified laboratory set-up and raised awareness on the potential impact of user-induced pressure variations on the integrity of minor elements. In a later paper based on laboratory tests and numerical modelling, Lee [49] focused on the T-junction connecting a DN40 PVC SL with a main pipe, confirming that the presence of a leakage near the junction can have a dampening effect on the transient pressure peaks.

Successively, Meniconi et al. [24,25] conducted laboratory tests to analyse the dynamic response of a looped system to transients caused by a change in water consumption. From an operational standpoint, transients were generated at the downstream end of a 25 m-long DN 25 HDPE SL, near the water meter, whereas PS was not fully reproduced. The combined effect of simultaneous users' activity was analysed and it emerged that (*i*) the most stressed parts of the WDN are those with the smaller diameters, regardless of where the transient is generated, and (*ii*) cavitation can occur, especially if the discharge in the SL is large.

More recently, in the only example of study focusing on users' induced pressure transients based on field monitoring [23], the effects of user's activity were investigated on a real 4 m-long DN20 PE SLs. The study revealed that the SL can be continuously affected by pressure variations that are more significant during the diurnal hours, whereas they are reduced at night. These pressure variations are generated not only by in-house devices, but also externally to the user. However, in the case of Marsili et al. [23], it was possible to consider only two measurement sections (one along the SL and one in the main WDN) due to accessibility reasons, and this led to a significant gap of knowledge concerning the pressure variation travelling along the PS. In addition, the determination of PS characteristics (i.e. diameters, materials, length) was hindered by the in-wall installation and this lack of information limited the complete interpretation of results. Therefore, ensuring controlled and reproducible measurements under real-world conditions remains challenging, highlighting the need for further methodological development. While existing literature acknowledges pressure transients induced from domestic device activation, detailed investigations of pressure waves generated specifically within minor systems are still lacking. Therefore, this study addresses this gap by examining user-induced pressure variations in a highly controlled laboratory setting, enabling a comprehensive and low-uncertainty characterization of pressure wave dynamics in minor systems.

This research investigates pressure waves generated in SLs and PSs

due to domestic devices activation using a full-scale, highly instrumented laboratory facility developed at the Water Engineering Laboratory (WEL) of the University of Perugia (Italy). The experimental set-up reproduces a complete SL and a connected domestic PS featuring four discharge points, each equipped with a custom-built manoeuvring apparatus to ensure repeatable test conditions. The influence of SL characteristics (i.e., diameter and material) on pressure wave propagation was examined by testing four different SL configurations, while the effect of device location was also investigated. The paper is organized as follows: Section 2 describes the experimental set-up, the hydraulic variables adopted, and the transient tests; Section 3 presents and discusses the results; and Section 4 provides the main conclusions and outlines future research directions.

2. Materials and methods

This section describes the experimental set-up installed at the WEL and the executed tests. Moreover, the reference quantities and the Lagrangian model adopted are introduced.

2.1. Experimental set-up

A full-scale (i.e. 1:1 scale) hydraulic set-up was constructed at the WEL of the University of Perugia. It replicates the main features of the real PS presented by Marsili et al. [23], reflecting the pipe lengths, diameters, and materials encountered in real-world installations and in full alignment with technical standards adopted in the field. Regarding the connections between the SL and the main network and between the PS and the domestic devices – elements that may induce significant head losses under steady-state conditions, as demonstrated by Karpenko [46] through CFD simulations – a tee junction was considered in all cases. This choice reflects the experimental objective, which was to investigate the role of the SL in the interaction mechanisms between the PS and the main network during transient events, rather than to optimize connection characteristics under steady-state conditions.

The set-up – the layout of which is schematically shown in Fig. 1 – consists of: (*i*) a pressurised supply tank providing a pressure head of about 20 m; (*ii*) a 120 m DN110 HDPE transmission main that feeds the SL through a tee connection; (*iii*) a 12 m interchangeable SL segment selected from four industry-standard pipe classes that collectively span the range of diameters and materials most frequently encountered in practice [50]. In greater detail, nominal diameters range from DN22 to

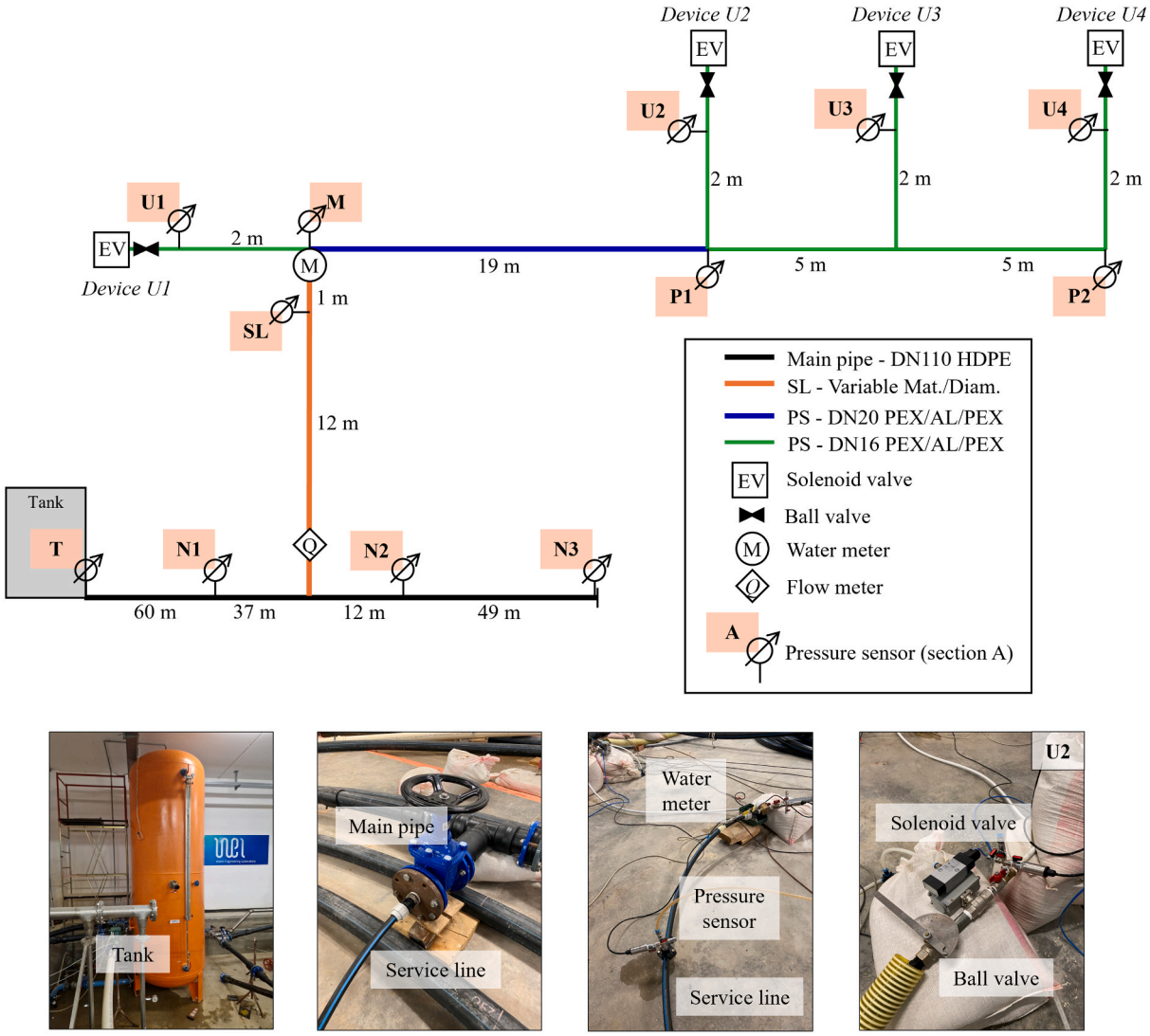


Fig. 1. Schematic layout (not in scale) of the set-up at WEL. Maneuver points (U1-U4) are represented by the coupling of a solenoid valve and a ball valve. The installation of the manoeuvring apparatus at U2 is pictured in the bottom-right panel, as an example. Measurement sections are marked by the "Pressure sensor" symbol and the corresponding section label.

DN40, while the materials used are HDPE, LDPE, and copper; (*iv*) a branched PS assembled from PEX/Al/PEX multilayer pipes (20 m DN20 followed by 10 m DN16 plus four 2 m DN16 branches), representative of contemporary residential installations; (*v*) a mechanical water meter placed at the SL–PS tee junction interface (i.e. section M), as typically found in real systems, and potentially representing a source of wave interaction; and (*vi*) four devices (U1–U4) equipped with custom-built manoeuvring apparatus featuring a ball valve for accurate discharge regulation and a normally-open solenoid valve for transient generation, with manoeuvring time of about 0.03 s.

It is acknowledged that the duration and profile of valve manouvre is a critical factor influencing the development of the initial pressure peak [51]. In this regard, valve operations at the household scale, particularly those involving manually operated domestic ball valves, exhibit highly variable opening and closure profiles and manoeuvring times, typically ranging between 0.2 s and 0.5 s [34]. However, the main goal of this laboratory investigation was not to characterize the stochastic nature of real-world user demand. Instead, fast manoeuvring time of the solenoid valves was adopted to isolate the propagation mechanisms of well-defined and repeatable pressure transients. Furthermore, this fast-manouvre scenario simulates the operation of common automatic devices (e.g., irrigation timers and solenoid valves in washing machines and dishwashers), thus maintaining relevance to a significant class of demand-induced transients.

High-frequency pressure signals, h, (i.e. the pressure-head time series) were acquired at twelve strategic locations throughout the experimental set-up by using piezoresistive pressure transducers (DRUCK® UNIK5000; full scale (FS) range: 4 to 25 bar; accuracy: ±0.2 %FS): the supply tank (T); three locations along the transmission main (N1–N3); a section along the service line (SL) located 1 m upstream of the SL–PS tee; immediately upstream of the meter (M); the four domestic devices (U1–U4); the reduction from DN20 to DN16 in the plumbing system (P1); and an additional section adjacent to outlet U4 (P2). An electromagnetic flowmeter (ISOIL® MS501; FS: 2.5 L/s; accuracy: ±0.2 %FS) downstream of the SL tee recorded the inlet discharge, Q.

Analog signals from the pressure sensors were digitized with an acquisition frequency of 2 kHz via National Instruments® modules. This acquisition frequency – corresponding to a sampling interval of $5{\cdot}10^{-4}$ s – was chosen to be sufficiently fine to accurately grasp pressure waves traveling within the system, which is characterized by short pipe lengths (i.e. 10^{0}-10^{1} m) and heterogeneous wave speeds (ranging from 200 to 1220 m/s). In addition to this, the response time of the pressure sensors (i.e. 3.5 kHz) significantly exceeded the acquisition frequency, ensuring that the pressure sensors are capable of capturing the fast pressure transients travelling in the pipe system. Concerning the flowmeter, a lower acquisition frequency (i.e. 1 Hz) was adopted. Specifically, flow-rate data were used for the calibration of the ball valves opening at the four discharge points under steady-state conditions, whereas they were not employed for the characterisation of the minor system under unsteady-state conditions. The entire acquisition and solenoid valve maneuvers were handled by custom software.

Table 1 summarises the SL characteristics: nominal diameter, DN, internal diameter, D, wall thickness, e, and pressure wave speed, a; in particular, for HDPE and LDPE pipes values are provided by Pothof & Karney [52], whereas for the copper pipe value is given by [53].

In contrast to SL materials, the PS is made of PEX/Al/PEX, a multilayer pipe consisting of an aluminium (Al) core bonded between two cross-linked polyethylene (PEX) layers. The Al layer raises pressure/temperature resistance and acts as an oxygen barrier, though the material is expensive and needs specialised installation [54,55]. According to technical datasheets, these pipes withstand up to 30 bar at 20 °C and 10 bar at 95 °C.

Table 1
Characteristics of the 12 m service line (SL) pipes.

Material	DN (mm)	D(mm)	e(mm)	a(m/s)
HDPE	25	19	3	300
	40	32	4	300
LDPE	25	19	3	200
Copper	22	20	1	1220

Since pressure wave speed data for PEX/Al/PEX pipes are not available in the literature, this parameter was experimentally assessed by measuring pressure wave travel times. Operationally, DN16 and DN20 PEX/Al/PEX segments were separately considered. Specifically, for each diameter, a 50 m-long segment was installed in a reservoir-pipe-valve layout. The downstream end of each segment was equipped with a solenoid valve to generate a fast closure, thereby inducing a sharp pressure transient. Pressure data were recorded at the downstream section of the pipe (i.e. in the proximity of the actioned valve). The induced pressure wave travelled back and forth along the 50 m pipe segment multiple times and this allowed the repeated evaluation of the pipeline's theoretical period, $T_{th} = 4L/a$, where L is the length of the pipe [56]. The wave speed was then assessed by considering the average of the experimental values of the theoretical period obtained which proved to be nearly constant for both diameters. The resulting value of a for DN16 and DN20 pipes is 630 m/s and 445 m/s, respectively. These results indicate that PEX/Al/PEX behaviour is comparable to that of PVC pipes in terms of wave speed. The relatively high values of a, larger than those expected for polyethylene pipes due to the presence of the aluminium core, together with the negligible variation in theoretical period values, suggest that viscoelastic effects are weak. [57–62].

To ensure stable and reliable testing conditions, a suitable preparatory phase was carried out as a preliminary part of the experimental methodology adopted. Specifically, before starting the transient tests, the system was operated under steady-state conditions for several days by maintaining a simultaneous outflow through all four discharge points. This procedure was replicated before testing each installed SL segment to achieve two prerequisites for the accurate characterization of hydraulic transients: (*i*) the de-aeration of the pipe system, and (*ii*) the establishment of the thermal equilibrium between the circulating water and the pipes. Operationally, during the tests conducted, water temperatures ranged from 15.9 to 16.8 °C.

2.2. Reference quantities

To compare tests characterized by different steady-state discharges, pressure-head variations were first evaluated as:

$$\Delta h = h - h_0 \tag{1}$$

where h_0 is the steady-state pressure head measured before transient generation. The dimensionless pressure signal, h^*, is then defined as:

$$h^* = \frac{h - h_0}{h_{max} - h_0} \tag{2}$$

with h_{max} being the first pressure peak recorded at the section where the maneuver was executed. A further subscript identifies the measurement section; for instance, the series at section SL is denoted as h_{SL}.

To identify the most stressed portions of the network during the transient, the cumulative hoop stress to which the pipe is subjected was evaluated from Mariotte-Barlow's equation [24]:

$$\sigma(t) = \frac{\sum_{\tau=0}^{t} |h(\tau) - h(t_{end})| D\gamma}{2e} \tag{3}$$

where t ranges from the beginning of the maneuver ($t = 0$) and t_{end}, the time required to the pressure signal to stabilize around a constant value $h(t_{end})$, and γ is the liquid specific weight. This cumulative definition departs from traditional approaches, which evaluate hoop stress for a single pressure value (often the peak during the first cycle). Specifically, summation over the entire window accounts for the full sequence of pressure fluctuations until stabilization around $h(t_{end})$. It therefore re-

sults that, for a given pipe, σ condenses the overall solicitation experienced during a test into a single indicator, facilitating the comparison of different transient scenarios.

2.3. The Lagrangian model

To interpret and theoretically validate the network dynamics observed during the first phase of the transients, a Lagrangian model was employed. This model solves the differential equations governing frictionless transients in elastic, pressurized pipes under the assumption of an instantaneous maneuver. By rigorously tracking pressure-wave propagation and interactions (e.g., at junctions, series connections, valves, and reservoirs), the Lagrangian approach provides the theoretical framework necessary to confirm the experimental results.

In greater detail, the Lagrangian model follows each incident wave F_j as it reaches a singularity along the j-th pipe, generating a reflected wave f_j (backward) and transmitted waves F_{Ti} in the i-th pipes, with $i \neq j$. For a generic junction, reflection and transmission coefficients are defined as [63,64]:

$$C_t = \frac{F_{Ti}}{F_j} = \frac{2\frac{\Omega_j}{a_j}}{\sum_{i=0}^{n_p}\frac{\Omega_i}{a_i}} \tag{4}$$

$$C_r = \frac{f_j}{F_j} = C_t - 1 \tag{5}$$

In Eqs. (4) and (5), Ω represents the cross-sectional area of the pipe whereas n_p is the number of pipes merging in the junction. From an operational standpoint, a reservoir can be treated as a pipe with $\Omega \to \infty$, resulting in in $C_t = 0$ and $C_r = -1$. In addition, in the case of a dead-end or a fully closed valve, flow is equal to zero, resulting in $C_t = 0$ and $C_r = 1$.

2.4. Series of transient tests executed at WEL

For each of the four pipes installed to reproduce the SL, opening and closure manoeuvres were executed at devices U1, U2, U3 and U4 by means of the manoeuvring apparatus developed, yielding to 16 tests (Table 2). Devices were activated one at a time via the solenoid valve, while all the others remained closed.

Each test was conducted twice to verify repeatability; in the following, the repeats are labelled "a" and "b" (e.g. Test #1a and Test #1b). The total duration of each test was 6 min, divided into three consecutive 2-min periods: (*i*) 0–2 min: all devices closed, with steady-state conditions; (*ii*) at $t = 2$ min, the solenoid valve was rapidly opened, generating the first pressure transient; (*iii*) 2–4 min: pressure was allowed to stabilise; (*iv*) at $t = 4$ min, the valve was then closed, producing a second transient; (*v*) 4–6 min: after the closure, the system returned to a steady-state behaviour comparable with the initial one. For brevity and clarity, the present analysis focuses on valve closure manoeuvres, as these produced the most severe pressure changes. In light of this, $t = 0$ corresponds to step (*iv*).

To isolate the effects of SL material/diameter and active device location, the same initial discharge was imposed in each test ($Q_0 = 0.26$ L/s), which is representative of typical domestic demand [2,65]. For each SL/device combination, the ball valve opening was adjusted to ensure the same value of the steady-state discharge, regardless of device location or SL configuration.

Table 2
Transient test configurations.

Test #	SL type	Transient generation device
1	DN22 Copper	U1
2		U2
3		U3
4		U4
5	DN25 HDPE	U1
6		U2
7		U3
8		U4
9	DN25 LDPE	U1
10		U2
11		U3
12		U4
13	DN40 HDPE	U1
14		U2
15		U3
16		U4

3. Results and discussion

The results obtained are discussed below, focusing on four main aspects: (*i*) test repeatability and magnitude of pressure variations induced by devices activation in the laboratory system, (*ii*) effect of the location of the device activated in the PS on the generated pressure wave, (*iii*) effect of SL characteristics in terms of pressure transient severity in the SL (i.e. section SL) and the main network (i.e. section N1), and (*iv*) cumulative hoop stress evaluation.

3.1. Magnitude of pressure variations and test repeatability

Test repeatability was first evaluated by comparing pressure signals from repeated closure manoeuvres. As an example, Fig. 2a and 2b show pressure values recorded during Tests #2a and #2b (valve closure at U2) and Tests #3a and #3b (closure at U3), respectively, with DN22 copper pipe as SL. In each case, the nearly overlapping pressure-head time series at all measurement sections over the analysed time window confirms good repeatability of the transient test conducted and data reliability.

A qualitative analysis of the signals reveals that the manoeuvres induce significant pressure variations. Pressure peaks reaching 150 m are very frequent and values exceeding 200 m occur inside the PS (sections U1, U2, U3 and U4). In the most stressed sections, these values approach the nominal pressure of the PEX/Al/PEX pipe (30 bar at 20 °C), raising the risk of damage in case of frequently recurring water hammer. It is worth noting that fitting elements are even more vulnerable: their nominal pressure is typically lower (about 10 bar at 20 °C), and improper installation can further reduce resistance. Notably, Fig. 2b indicates that the largest variation does not appear at the generation point (i.e. device U2), but at an adjacent section.

Pressure oscillations are also evident in the SL (i.e. section SL, green line in Fig. 2), with variations of about 50 m. Conversely, only a small portion of the pressure wave (in the order of a few meters) reaches the main network (i.e. section N1, dark red line in Fig. 2). Comparable results were observed for the other three SL types.

It is important to emphasize that the scenario reproduced at WEL is realistic. The discharge imposed by means of the ball valve ($Q_0 = 0.26$ L/s) corresponds to typical domestic water use, while the rapid maneuver of the solenoid valve mimics automatic appliance withdrawals, such as those from washing machines. Consequently, the observed phenomenon is highly relevant, as it could affect any SL supplied by a WDN, and warrants further investigation due to its potential role in pipe failure.

The analysis also reveals that relying on a single pressure time series (typically acquired in relation to the transient generation section) is an overly simplistic approach for assessing system dynamics. While practical field constraints might often force this choice, such a limited perspective may fail to capture the complex phenomena of wave propagation and energy dissipation throughout the network. Therefore, measuring pressure at multiple sections within a controlled laboratory environment proves invaluable, providing comprehensive data required to accurately interpret how pressure fluctuations evolve.

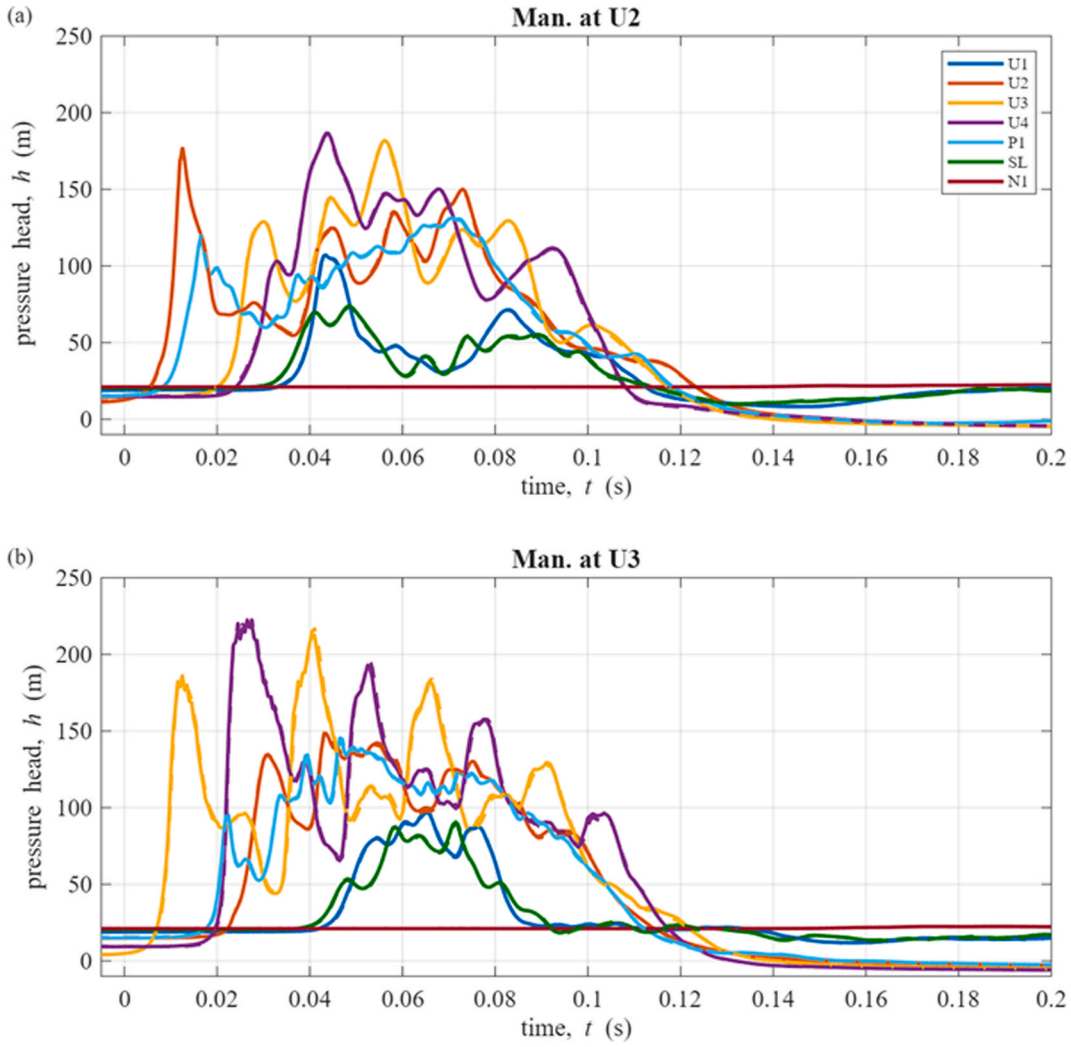


Fig. 2. Pressure signals acquired at measurement sections during a closure maneuver executed at: (a) U2 (Test #2a with solid line and Test#2b with dashed line), and (b) U3 (Test #3a with solid line and Test #3b with dashed line).

3.2. Role of device location

The following analysis explores how the location of the activated device in the PS affects pressure wave propagation throughout the PS, the SL, and the main network. To compare pressure signals in sections U1-U4 (in the plumbing system), SL (along the service line), and N1 (in the main network), h^* defined in Eq. (2) is used. As in Section 3.1, closures of U1-U4 were analysed for the DN22 copper SL as a representative case. Comparable results were obtained for other SL types. The four panels in Fig. 3 correspond to closure at U1 (Fig. 3a), U2 (Fig. 3b), U3 (Fig. 3c), and U4 (Fig. 3d). For closure at U1 (Fig. 3a), U4 is more stressed than U2 and U3, due to its terminal location.

Overall, the analysis reveals that, when the maneuver moves towards the downstream end of the PS (i.e. it is generated at U2, U3 and U4), the initial pressure variation tends to persist into the system which results more solicited with respect to the case of the manouvre generated at U1. In addition, the most stressed section is not necessarily the one where the transient is generated, but often it is an adjacent branch near a dead end. For example, in Fig. 3d the closure at U4 yields the highest peak at U3, 1.6 times the peak at U4. Moreover, the first peak (i.e. the peak observed during the first transient cycle) is not always the largest observed in a section, so referring only to the first pressure variation at the maneuver section as a safety reference can be misleading.

Finally, the results indicate that, while the SL experiences pressure variations amounting to approximately 40–50 % of the incident wave regardless of the maneuver location, the response of the PS is highly dependent on this. Notably, the terminal sections of the PS are systematically the most stressed. This finding is particularly relevant, as domestic PSs commonly have branched layouts due to technical and economic aspects. Similar trends were observed across all tested SL types.

3.3. Role of SL characteristics

The influence of SL material and diameter on transient response is analysed by iteratively replacing the SL segment in the laboratory set-up. As a representative case, the closure maneuver at location U1 is considered for all four SL types (Tests #1, #5, #9 and #13).

Fig. 4 presents the time series of pressure-head variation, Δh, at sections U1, SL, and N1. This figure reveals that the closure at location U1 generates a pressure variation of about 180 m with the same waveform in all SL configurations. Achieving this similarity, despite repeated SL replacements, was crucial for ensuring a meaningful and reliable comparison of the data.

Specifically, the pressure wave generated at U1 propagates along the PS toward the PS-SL junction, then it travels along the SL to the SL-main network junction. Understanding the propagation mechanisms of pressure waves from the PS to the SL and, subsequently, to the main network

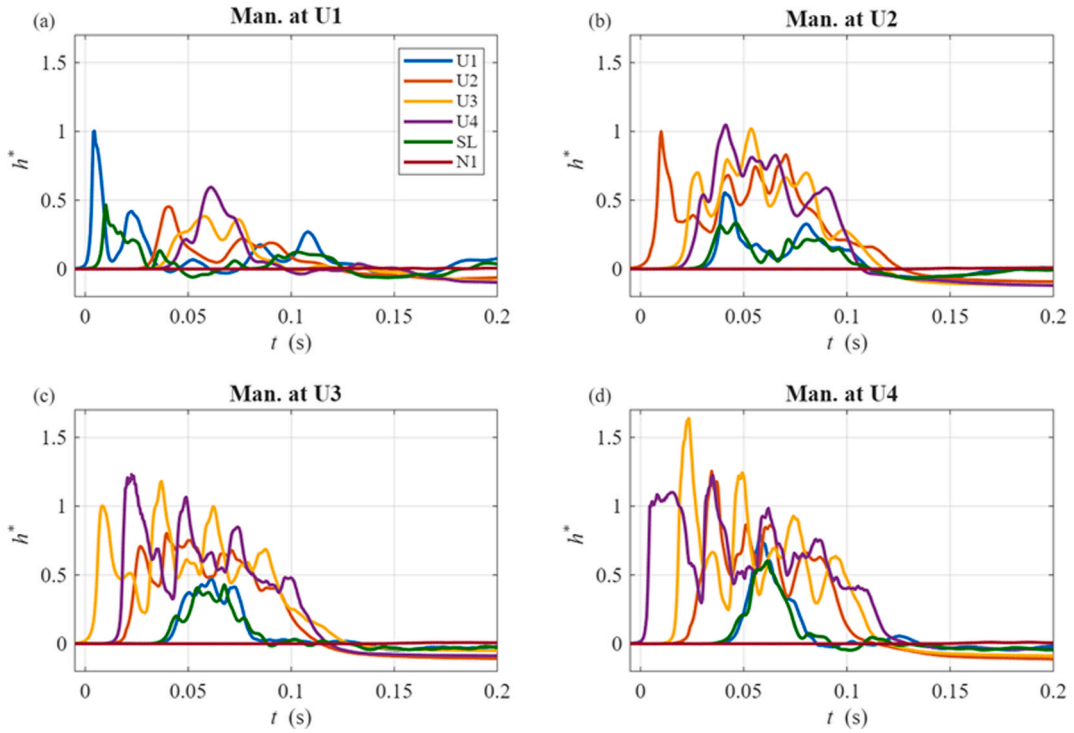


Fig. 3. Pressure signals acquired at the measurement sections U1, U2, U3, U4, SL and N1 during a closure maneuver executed at: (a) U1 (Test #1), (b) U2 (Test #2), (c) U3 (Test #3), and (d) U4 (Test #4).

requires the analysis of wave interactions at each junction. These interactions can be described by the Lagrangian model introduced in Section 2.3, along with the coefficients of transmission C_t and reflection C_r, defined in Eqs. (4) and (5), respectively.

For the sake of clarity, the PS and the main network are treated as fixed components – specifically, a DN20 PEX/Al/PEX pipe with $a = 445$ m/s, and a DN110 HDPE pipe with $a = 400$ m/s, respectively) – while only the SL properties are varied. In addition, the junctions are intentionally simplified in this analysis – most notably the PS-SL junction, which omits the DN16 branch feeding U1 – to provide a clear picture of how a pressure wave behaves when it reaches the interfaces between the PS and the SL, and the SL and the main network.

For the PS-SL junction, the calculated C_t (Fig. 5a) values show that in an extreme combination of small-diameter and high pressure wave speed of the SL (e.g. DN22 copper) the transmitted wave may even exceed the incident one (C_t higher than 1). For this combination, also the value of C_r (shown in Fig. 5b) is greater than 0, meaning a further increase of the pressure in the PS. In other words, a "magnification zone" appears, a situation that should be avoided – especially given copper's widespread use for SL replacements in countries such as the United States [50]. At the opposite extreme, a large diameter combined with a low pressure wave speed of the SL (e.g. DN40 HDPE) produces C_t approaching 0 and C_r tending to −1. In other words, almost the entire incident wave is reflected, causing a pronounced pressure drop in the PS while leaving the SL largely unaffected.

Consistent with theory, the DN22 copper SL experiences the largest pressure variations; DN40 HDPE the smallest; DN25 LDPE and DN25 HDPE fall in between (Fig. 6a, 6b, and 6c). Although the transient originates in the PS – specifically, not immediately downstream of the SL – the predicted hierarchy still emerges. Notably, this behaviour is independent of the manoeuvre's location, even though the most critical case is the closure at U4 (Fig. 6c), which is at the extreme downstream end of the PS.

The SL-main pipe junction exhibits behaviour according to C_t and C_r (Fig. 5c and 5d). A SL with a small D and large a (e.g. DN22 copper) transmits a small amount of the incident wave to the network (i.e. C_t approaches 0) while reflecting nearly the entire wave back toward the SL (C_r tends to −1). This configuration strongly excites the SL but effectively protects the main pipe. Conversely, a SL with a large D and small a causes a larger transmitted wave (C_t tends to 0.7) and a smaller reflected one (C_r tends to −0.3). In other words, metallic SLs with small D experience the greatest dynamic loading, whereas oversized plastic SLs experience the mildest stress condition even if they transfer more energy into the distribution main.

The experimental results confirmed the theoretical predictions. Notably, even under the worst-case configuration for the distribution network – an oversized plastic SL (e.g. DN40 HDPE SL) – the pressure variation measured at N1 remained minimal, limited to just a few meters (Fig. 6d, 6e, and 6f). In other words, although DN40 HDPE transmits the largest fraction of the wave to the main pipe, the absolute amplitude that reaches section N1 remains very limited. As a results, the network experiences only negligible fluctuations. Importantly, this behaviour is consistent regardless of maneuver location.

However, this outcome conflicts with the findings obtained with regard to steady-state conditions in relation to peak discharges. In particular, Douglas et al. [66] show that reducing SL diameter can offer both economic and hydraulic advantages while still complying with recommended velocity limit (< 3 m/s) and, thus, maintaining energy losses under control. In other words, the literature presents no unified guidance: design steady-state criteria favour smaller diameters, whereas the unsteady-state results from this study show that smaller SLs promote the transmission of the incident pressure wave, increasing pressure variations within the SL itself. Therefore, defining an optimal replacement strategy requires water utilities to balance both perspectives – steady-state capacity and transient resilience – rather than relying on a single design criterion.

3.4. Cumulative hoop stress evaluation

The final analysis compares the cumulative hoop stress, σ (t), experienced by section SL in relation to different SL material, diameter, and maneuver location. Fig. 7 shows the cumulative hoop stress σ for the

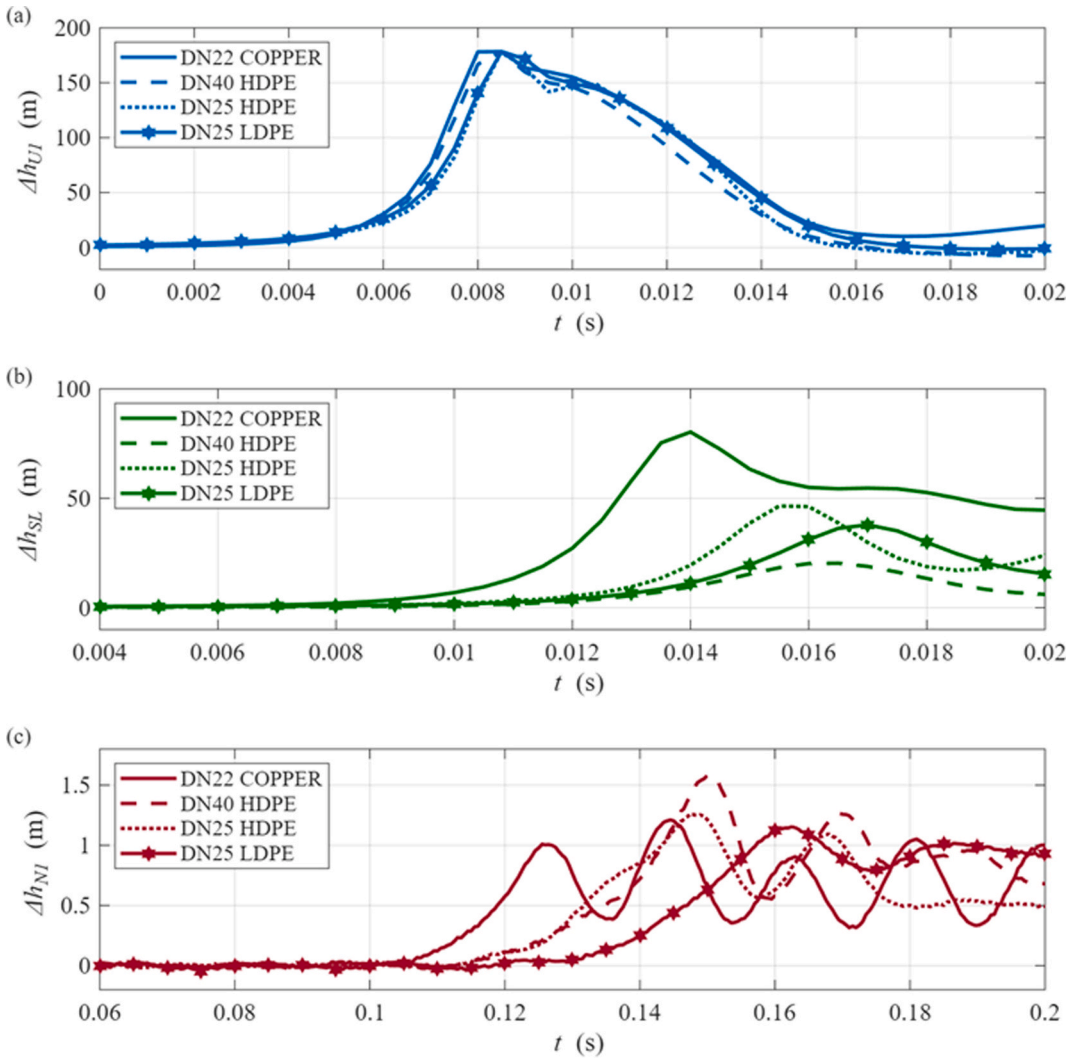


Fig. 4. Role of service line (SL) characteristics (i.e. material and diameter). Pressure-head variation time series at sections: (a) U1, (b) SL, and (c) N1 during the closure of device U1 for each of the four SL types (Tests #1, Tests #5, Test #9, and Test #13).

four SL types, in relation to two manoeuvres here considered as a reference: the former executed at U1 (panel a) and the latter executed at U3 (panel b).

For both closures, σ rises sharply during the first second, mirroring the initial pressure surge. The DN22 copper SL consistently records the highest stresses – exceeding $5{\cdot}10^5$ kPa after the U1 closure and $9{\cdot}10^5$ kPa after the U3 closure – whereas the polymeric SLs register roughly half these values. After this time, the curves adopt an almost horizontal trend in the face of pressure stabilization around the reference head (i.e. the final static pressure) and the system approaches a new steady-state condition; from this point, the stress does not significantly vary over time. Conversely, hoop-stress values are markedly higher when the valve is closed at U3 (located at almost downstream end of the PS) as opposed to U1 (just at the upstream end of the PS). This confirms that manoeuvres performed further downstream impose greater dynamic loading on the SL.

Overall, this analysis provides a clear, simple indicator to compare the transient response of different SL designs.

4. Conclusions

This research, conducted at the Water Engineering Laboratory (WEL) of the University of Perugia, explored pressure waves generated by domestic device activation, along with their propagation throughout plumbing systems (PSs) and service lines (SLs). Using a highly controlled and monitored full-scale laboratory set-up, the study simulated user activity by inducing discharge changes in the SL through the actuation of solenoid valves at different PS locations. High-frequency pressure data (i.e. 2 kHz) and flow rate in the SL were collected to thoroughly characterize the phenomenon. The research also investigated the impact of SL characteristics, such as diameter (DN22 to DN40) and material (copper and polymeric pipes), on transient response.

The key findings are summarized in the following.

- Independently of the SL configuration, significant pressure peaks (even larger than 200 m) were observed within the PS in face of a flow change in line with typical domestic water use. These values approach the nominal pressure of the PEX/AI/PEX pipes (30 bar at 20 °C), while exceeding the nominal pressure (around 10 bar at 20 °C) of hydraulic fittings installed to connect PEX/Al/PEX pipe segments. Pressure variations of about 50 m were evident in the SL, whereas fluctuations of only a few meters reached the main network.
- The location of the activated device significantly affects pressure wave propagation. Pressure wave severity increases as the location of the device activated moves toward the downstream end of the PS. Interestingly, the tests revealed that the most stressed section did not coincide with the point of transient generation, highlighting the importance of studying the phenomenon in a highly controlled

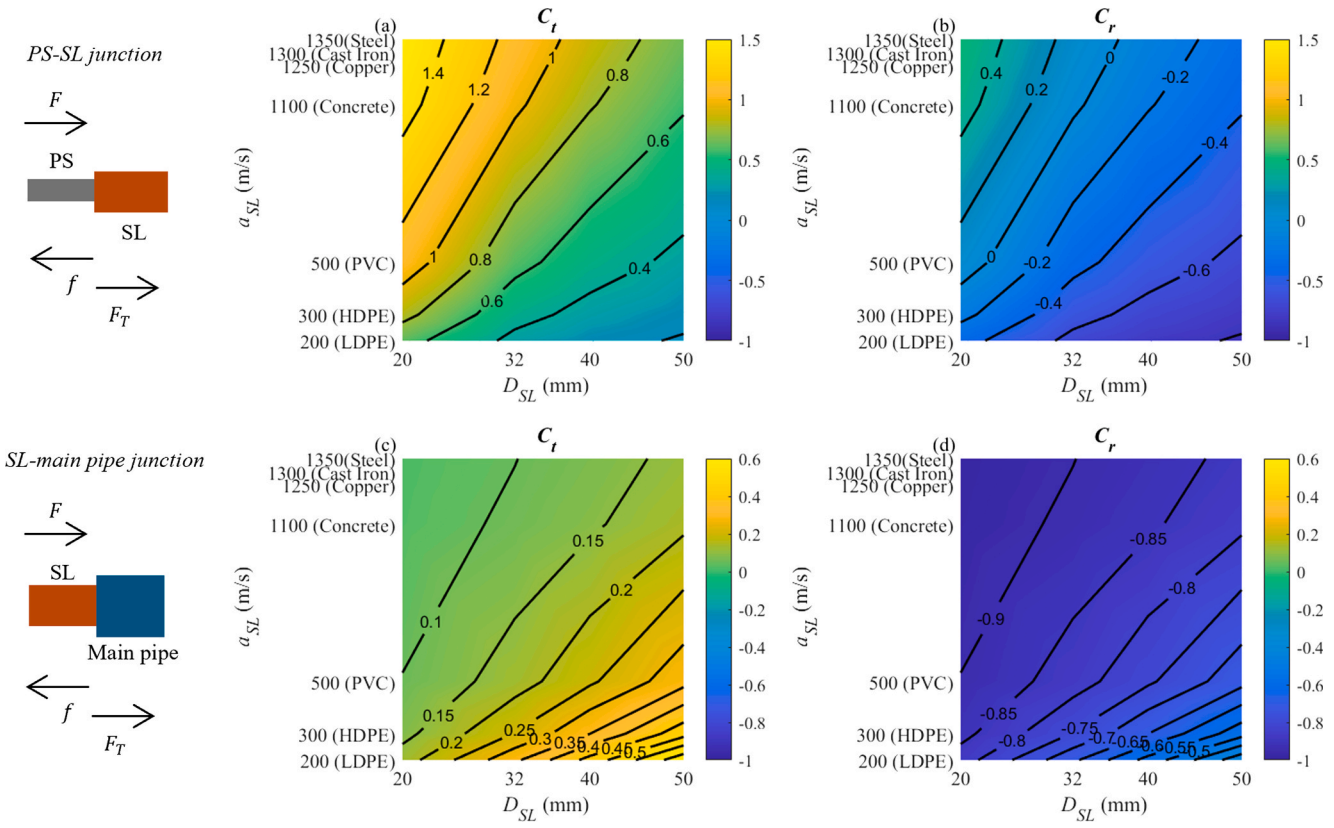


Fig. 5. Analytical transmission (C_t) and reflection (C_r) coefficients for an incident pressure wave, F, at two interfaces, as functions of service line (SL) diameter (D_{SL}) and material (i.e. pressure wave speed, a_{SL}). a) C_t at the plumbing system–service line (PS–SL) junction, b) C_r at the PS–SL junction, c) C_t at the SL–main pipe junction, and d) C_r at the SL–main pipe junction.

environment to unveil its nature. In general, the terminal branches of the PS experienced the greatest pressure variations, indicating them to be critical sections. In addition, the tests revealed that the first transient cycle doesn't always correspond to the largest observed pressure values, and consequently, taking it as a safety reference can be misleading.

- SL material and diameter significantly influence pressure wave propagation. Both the Lagrangian model and the experimental observations confirmed that, at the PS-SL junction, small-diameter, high pressure wave speed SLs (e.g. DN22 copper) could lead to a conservation of the incident wave in the transmitted one. Conversely, large-diameter, low pressure wave speed SLs (e.g. DN40 HDPE) caused most of the incident wave to be reflected into the PS, while the SL remained largely unaffected. At the SL-main pipe junction, small-diameter, high-wave-speed SLs transmitted a small amount of the wave to the network, reflecting it back in the SL. Vice-versa, large-diameter, low pressure wave speed SLs resulted in a larger wave transmitted to the main network. However, even with the worst-case scenario for the main pipe (i.e. oversized plastic SL), the magnitude of pressure variation at N1 remained negligible (i.e. few meters).
- The cumulative hoop stress confirms to be an effective quantity for comparing how different SL designs respond to transients. In this study, the highest cumulative hoop stresses values were consistently assessed in relation to DN22 copper SL, significantly exceeding those in polymeric SLs. Stresses were markedly higher when the valve was closed further downstream in the PS, confirming that manoeuvres performed further downstream impose greater dynamic loading on the SL.

The practical limitations of this experimental study concern two main aspects: the experimental set-up and the transient tests. Concerning the experimental set-up, while the materials, diameters, and the branched layout of the minor system fully align with typical field standards and replicate a real-world system [34], the set-up only considers a single PS supplied by a small portion of the main network (with fixed pipe characteristics) which is a simplification compared to a real-world system. In addition, the PS realized in the laboratory does not fully capture the complexity of all possible internal PSs, which can vary widely based on building size and device arrangement. Furthermore, the upstream boundary condition – a pressurized tank used to maintain constant downstream pressure – is just one of several possible real-world upstream scenarios that could affect transient behaviour. Regarding the transient tests, the main methodological limitation stems from the technique used to generate transients. The use of a fast-response solenoid valve was necessary to achieve sharp and repeatable transients for wave propagation analysis. This maneuver, however, inherently represents an upper bound on transient severity. While the fast closure time achieved is still compatible with the operational speed of automatic household appliances, such as washing machines or irrigation timers, typical real household manual valve operations feature a wide range of closure times and variable closure profiles. Consequently, the comprehensive investigation of more realistic maneuver and their effects on wave generation is reserved for future work.

In conclusion, this study reveals a conflict between steady-state design criteria (which might favour SLs with smaller diameter) and unsteady-flow conditions (demonstrating that small-diameter SLs can significantly amplify transients). In addition, while the study mainly focuses on the hydraulic results, the reliability and complexity of the experimental set-up and transient tests conducted provides valuable insights for researchers pursuing similar experimental campaigns.

Future research will be carried out to develop a comprehensive design framework (or an optimal replacement strategy) for SLs that effectively balances both steady-state capacity and transient resilience.

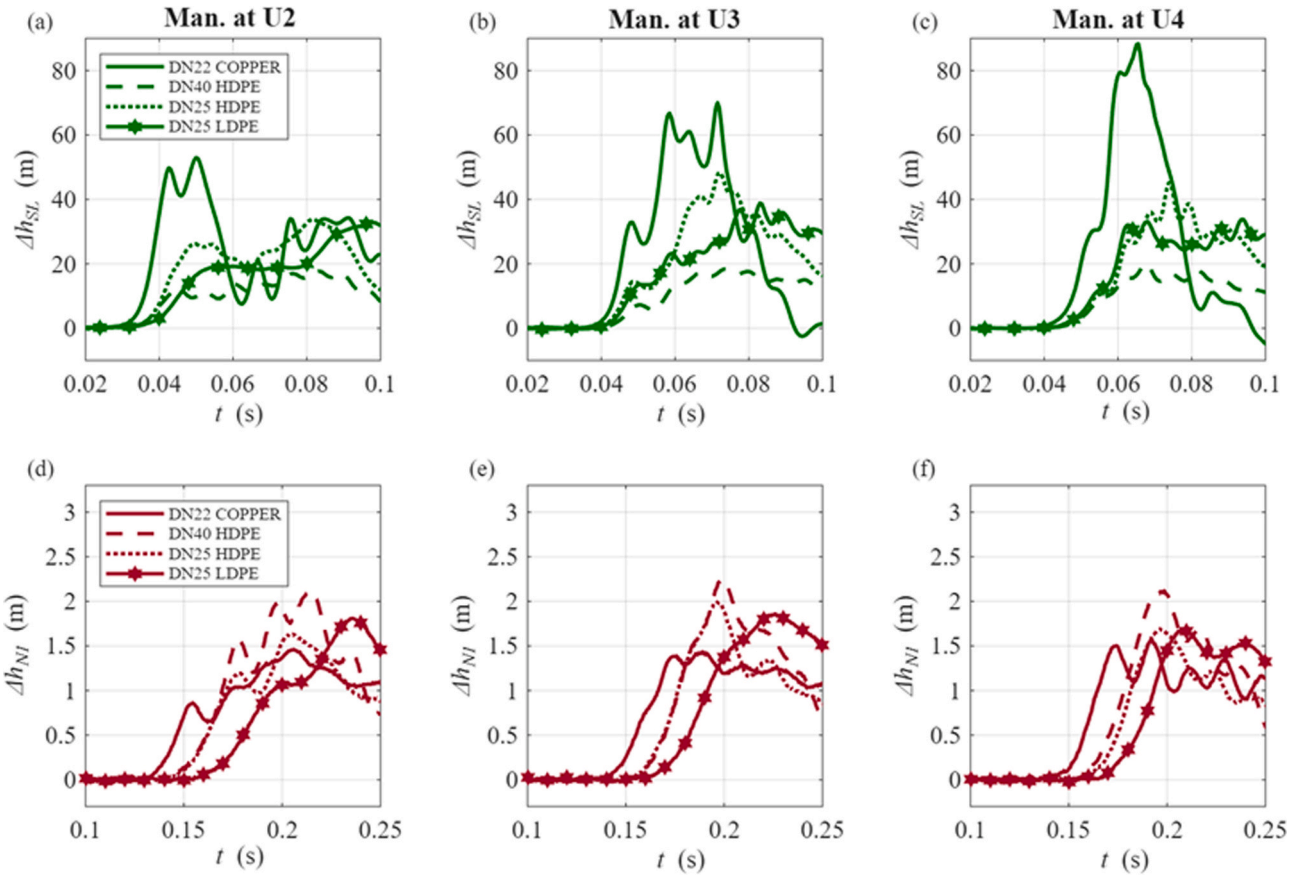


Fig. 6. Role of SL characteristics. Pressure-head variation time series at sections SL (subplots a–c) and N1 (subplots d–f) following closure of device U2 (a, d), U3 (b, e), and U4 (c, f), respectively; curves for all four SL types are shown in each subplot.

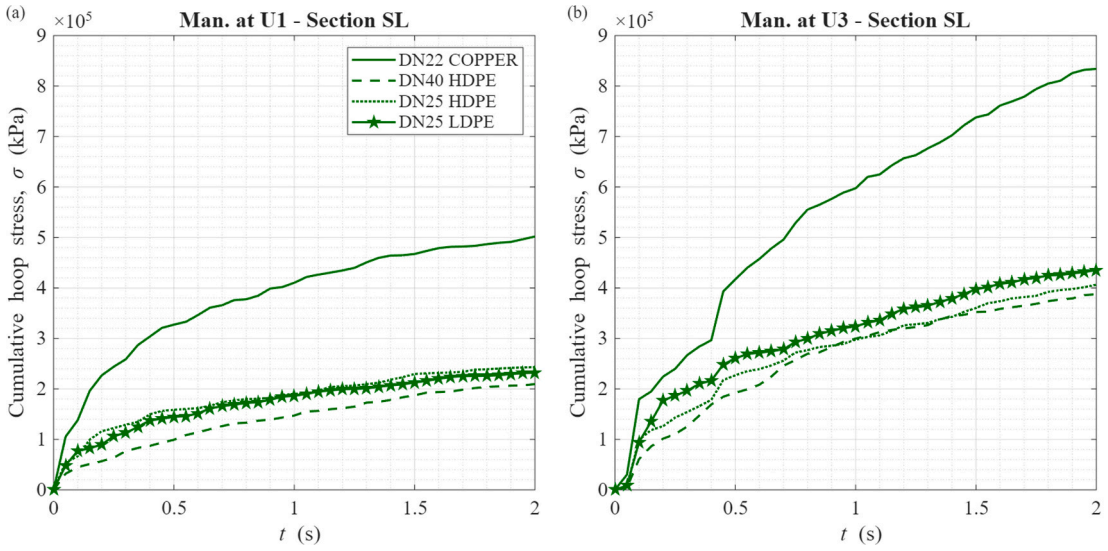


Fig. 7. Time series of the cumulative hoop stress, $\sigma(t)$, at section SL for the four service-line types following closure at (a) U1, and (b) U3.

Furthermore, there is a major need to focus on protecting the minor systems against these pressure fluctuations. This entails the development of techniques or devices to damp the effects of user-induced pressure transients at the building scale, considering the perspectives of both the final user and the water utility.

CRediT authorship contribution statement

Valentina Marsili: Writing – review & editing, Writing – original draft, Visualization, Validation, Software, Methodology, Investigation, Formal analysis, Conceptualization. **Debora Falocci:** Writing – review & editing, Writing – original draft, Validation, Software, Methodology, Investigation, Formal analysis, Data curation, Conceptualization. **Caterina Capponi:** Writing – review & editing, Writing – original draft,

Visualization, Validation, Software, Methodology, Investigation, Formal analysis, Data curation, Conceptualization. **Filippo Mazzoni:** Writing – review & editing, Writing – original draft, Methodology, Formal analysis. **Stefano Alvisi:** Writing – review & editing, Supervision, Resources, Project administration, Methodology, Funding acquisition, Formal analysis, Conceptualization. **Bruno Brunone:** Writing – review & editing, Supervision, Resources, Project administration, Funding acquisition. **Silvia Meniconi:** Writing – review & editing, Writing – original draft, Visualization, Validation, Supervision, Resources, Project administration, Methodology, Formal analysis, Conceptualization.

Declaration of competing interest

The authors declare that they have no known competing financial interests or personal relationships that could have appeared to influence the work reported in this paper.

Acknowledgments

This research has been jointly supported by the University of Perugia "Fondi di ricerca di Ateneo-edizione 2022"; by the European Union - Next Generation EU, Mission 4, Component 2 under the Project of Relevant Interest PRIN2022 (D.D. 104/2022 MUR) "Hybrid Transient-Machine Learning Approach for Anomaly Detection and Classification in Water Transmission Mains (TANDEM)" (project 2022FR5FB7; CUP: J53D23002110006).

This work was carried out within the project MORE4WATER, which has received funding from MUR (Italy), FCT (Portugal), Fapesc (Brazil), and the European Union's Horizon Europe Programme under the 2022 Joint Transnational Call of the European Partnership Water4All (Grant Agreement n° 101060874).

Data availability

Data will be made available on request.

References

[1] W. Zeng, J. Hu, B. Cui, Z. Yang, Z. Hu, C. Han, L. Bai, Hierarchical structure analysis of water distribution networks coupling pipeline dual graph and infomap algorithm, Reliab. Eng. Syst. Saf. 260 (2025) 110945, https://doi.org/10.1016/j.ress.2025.110945.

[2] F. Mazzoni, et al., Investigating the characteristics of residential end uses of water: a worldwide review, Water Res. 230 (2023) 119500, https://doi.org/10.1016/j.watres.2022.119500.

[3] A. Criminisi, C.M. Fontanazza, G. Freni, G. La Loggia, Evaluation of the apparent losses caused by water meter under-registration in intermittent water supply available to purchase, Water Sci. Technol. 60 (2009) 2373–2382, https://doi.org/10.2166/wst.2009.423.

[4] M. De Marchis, C.M. Fontanazza, G. Freni, G. La Loggia, E. Napoli, V. Notaro, Analysis of the impact of intermittent distribution by modelling the network-filling process, J Hydroinform 13 (2011) 358–373, https://doi.org/10.2166/hydro.2010.026.

[5] V. Marsili, F. Mazzoni, I. Marzola, S. Alvisi, M. Franchini, Intermittent water supply system rehabilitation through a multiphase methodology based on network analysis and hydraulic modeling, J. Water Res. Plan. Man. 149 (2023) 04023048, https://doi.org/10.1061/JWRMD5.WRENG-6116.

[6] X. Zhou, W. Yin, K. Yang, Adaptive acoustic leak location of long buried pipe via transient optimization statistical analysis, IEEE Trans. Instrum. Meas. 73 (2024) 3510110, https://doi.org/10.1109/TIM.2024.3353837.

[7] D. Vališ, K. Hasilová, M. Forbelská, Vintr Z Reliability modelling and analysis of water distribution network based on backpropagation recursive processes with real field data, Measurement 149 (2020) 107026, https://doi.org/10.1016/j.measurement.2019.107026.

[8] M.F. Ghazali, N.A. Said, M.H. Yusop, E. Erdiwansyah, Ramli MAP improved leak localization in water distribution systems using SGTCC: comparative analysis with EMD-HT and EEMD-HT under transient conditions, Measurement 118072 (2025), https://doi.org/10.1016/j.measurement.2025.118072.

[9] H. Liu, H. Fang, X. Yu, Adaptive water supply pipe leakage localization under low SNR based on GWO-VMD-CC, IEEE Trans. Instrum. Meas. 74 (2025) 9600415. https://ieeexplore.ieee.org/document/10907899.

[10] X. Meng, Z. Huang, Leakage detection and localization of buried water pipe using ground penetrating radar, Measurement 117902 (2025), https://doi.org/10.1016/j.measurement.2025.117902.

[11] R. Qi, D.R. Yntema, M. Cao, An Inline impedance-based leakage detection method for nonconducting buried water mains, IEEE Trans. Instrum. Meas. 74 (2025) 9507408. https://ieeexplore.ieee.org/document/10912704.

[12] M. Carratu, S.D. Iacono, G. Di Leo, V. Gallo, C. Liguori, A. Pietrosanto, Smart water meter based on deep neural network and undersampling for PWNC detection, IEEE Trans. Instrum. Meas. 72 (2023) 1002211, https://doi.org/10.1109/TIM.2023.3242018.

[13] A. Pietrosanto, M. Carratù, Liguori C sensitivity of water meters to small leakage, Measurement 168 (2021) 108479, https://doi.org/10.1016/j.measurement.2020.108479.

[14] Y.A. Le Gouellec, C.DA. Installation, Condition Assessment, and Reliability of Service Lines, AWWA Research Foundation, Denver (USA), 2007.

[15] J. Thornton, R. Sturm, G. Kunkel, Water Loss Control, McGraw-Hill, New York (USA), 2008.

[16] Resenterra M, Grata S, Alvisi S, Franchini M. Caratterizzazione dello stato strutturale di una rete acquedottistica attraverso la georeferenziazione delle rotture e l'analisi statistica, in: Proceedings of the Third Seminar "La ricerca delle perdite e la gestione delle reti di acquedotto" (Perugia, Italy) (2008).

[17] J. Gibson, B. Karney, Y. Guo, Predicting health risks from intrusion into drinking water pipes over time, J. Water Res. Plan. Man. 145 (2019) 04019001, https://doi.org/10.1061/(ASCE)WR.1943-5452.0001039.

[18] A. Colombo, B. Karney, Pipe breaks and the role of leaks from an economic perspective, Water Sci. Technol. Water Supply 3 (2003) 163–169, https://doi.org/10.2166/ws.2003.0099.

[19] P.W. Mayer, W.B. DeOreo, D.M. Lewis, Seattle Home Water Conservation Study: the Impacts of High Efficiency Plumbing Fixture Retrofits in Single-Family Homes, Aquacraft Inc., Boulder (USA), 2000.

[20] W.B. DeOreo, P.W. Mayer, L. Martien, M. Hayden, A. Funk, M. Kramer-Duffield, R. Davis, J. Henderson, B. Raucher, P. Gleick, M. Heberger, California Single Family Home Water Use Efficiency Study, Aquacraft Inc., Boulder (USA), 2011.

[21] W.B. DeOreo, P.W. Mayer, B. Dziegielewski, J. Kiefer, Residential End Uses of Water, Water Research Foundation, Denver (USA), 2016.

[22] J. Latif, M.Z. Shakir, N. Edwards, M. Jaszczykowski, N. Ramzan, V. Edwards, Review on condition monitoring techniques for water pipelines, Measurement 193 (2022) 110895, https://doi.org/10.1016/j.measurement.2022.110895.

[23] V. Marsili, F. Mazzoni, S. Alvisi, F. Maietta, C. Capponi, S. Meniconi, B. Brunone, M. Franchini, Investigation of pressure transients induced on a real water service line by user's activity, AQUA – Water Infrastruc. Ecosyst. Soc. 72 (2023) 2331–2346.

[24] S. Meniconi, F. Maietta, S. Alvisi, C. Capponi, V. Marsili, M. Franchini, B. Brunone, Consumption change-induced transients in a water distribution network: laboratory tests in a looped system, Water Resour. Res. 58 (2022) e2021WR031343, https://doi.org/10.1029/2021WR031343.

[25] S. Meniconi, F. Maietta, S. Alvisi, C. Capponi, V. Marsili, M. Franchini, B. Brunone, A quick survey of the most vulnerable areas of a water distribution network due to transients generated in a service line: a Lagrangian model based on laboratory tests, Water 14 (2022) 2741, https://doi.org/10.3390/w14172741.

[26] N.A. Barton, T.S. Farewell, S.H. Hallett, T.F. Acland, Improving pipe failure predictions: factors affecting pipe failure in drinking water networks, Water Res. 164 (2019) 114926, https://doi.org/10.1016/j.watres.2019.114926.

[27] A.J. Hoskins, Monitoring the Hydraulic Dynamics in Water Distribution Systems, Imperial College, 2015. PhD Thesis;.

[28] D. Starczewska, R. Collins, J. Boxall, Transient behavior in complex distribution network: a case study, Procedia Eng. 70 (2014) 1582–1591, https://doi.org/10.1016/j.proeng.2014.02.175.

[29] D. Starczewska, R. Collins, J. Boxall, Occurrence of transients in water distribution networks, Procedia Eng. 119 (2015) 1473–1482, https://doi.org/10.1016/j.proeng.2016.01.001.

[30] S. Rathnayaka, B. Shannon, P. Rajeev, J. Kodikara, Monitoring of pressure transients in water supply networks, Water Resour. Manag. 30 (2015) 471–485, https://doi.org/10.1007/s11269-015-1172-y.

[31] V. Marsili, S. Meniconi, S. Alvisi, B. Brunone, M. Franchini, Experimental analysis of the water consumption effect on the dynamic behaviour of a real pipe network, J. Hydraul. Res. 59 (2021) 477–487, https://doi.org/10.1080/00221686.2020.1780506.

[32] C. Capponi, D. Falocci, B. Brunone, X. Yu, C. Yu, S. Meniconi, Pump operations-induced transients in water distribution systems, Lab. Exp. Phys Fluids 37 (2025) 037155, https://doi.org/10.1063/5.0253423.

[33] A. Haghighi, Analysis of transient flow caused by fluctuating consumptions in pipe networks: a many-objective genetic algorithm approach, Water Resour. Manag. 29 (2015) 2233–2248, https://doi.org/10.1007/s11269-015-0938-6.

[34] V. Marsili, S. Meniconi, S. Alvisi, B. Brunone, M. Franchini, Stochastic approach for the analysis of demand induced transients in real water distribution systems, J. Water Res. Plan. Man. 141 (2022) 04021093, https://doi.org/10.1061/(asce)wr.1943-5452.0001498.

[35] S. Meniconi, A. Rubin, L. Tirello, A. Doro, B. Brunone, C. Capponi, Mapping pressure surge source in urban water networks: Integrating low- and high-frequency pressure data with an illustrative real case study, Water Resour. Res. 60 (2024) e2023WR036773, https://doi.org/10.1029/2023WR036773.

[36] H. Rezaei, B. Ryan, I. Stoianov, Pipe failure analysis and impact of dynamic hydraulic conditions in water supply networks, Procedia Eng. 119 (2015) 253–262, https://doi.org/10.1016/j.proeng.2015.08.883.

[37] I. Stoianov, A. Hoskins. Cumulative pressure induced stress for characterising pressure transients and variability in water supply networks, in: Proceedings of the International Conference on Computing and Control in the Water Industry (Sheffield, UK) 2017. doi: 10.15131/shef.data.5364700.v1.

[38] C. Jara-Arriagada, I. Stoianov, Pipe breaks and estimating the impact of pressure control in water supply networks, Reliab. Eng. Syst. Saf. 210 (2021) 107525, https://doi.org/10.1016/j.ress.2021.107525.
[39] C. Jara-Arriagada, I. Stoianov, High resolution water pressure monitoring for the assessment of fatigue damage in water distribution pipes, in: Proceedings of the 2nd International Join Conference on Water Distribution System Analysis & Computing and Control in the Water Industry (Valencia, Spain) (2022), pp. 1220-1235.
[40] M. Stosiak, I. Yatskiv, O. Prentkovskis, M. Karpenko, Reduction of pressure pulsations over a wide frequency range in hydrostatic systems, Machines 13 (2025) 25, https://doi.org/10.3390/machines13010025.
[41] P.F. Boulos, B.W. Karney, D.J. Wood, S. Lingireddy, Hydraulic transient guidelines for protecting water distribution systems, J. Am. Water Works Assoc. 97 (2005) 111–124, https://doi.org/10.1002/j.1551-8833.2005.tb10892.x.
[42] H. Rezaei, Impact of pressure fluctuations on pipe failures in water distribution networks, Imperial College, 2017. PhD Thesis.
[43] C. Jara-Arriagada, I. Stoianov, Pressure-induced fatigue failures in cast iron water supply pipes, Eng. Fail. Anal. 155 (2024) 107731, https://doi.org/10.1016/j.engfailanal.2023.107731.
[44] C. Konstantinou, C. Jara-Arriagada, I. Stoianov, Investigating the impact of cumulative pressure-induced stress on machine learning models for pipe breaks, Water Resour. Manag. 38 (2024) 603–619, https://doi.org/10.1007/s11269-023-03687-7.
[45] X. Fan, X. Zhang, X.B. Yu, Uncertainty quantification of a deep learning model for failure rate prediction of water distribution networks, Reliab. Eng. Syst. Saf. 236 (2023) 109088, https://doi.org/10.1016/j.ress.2023.109088.
[46] M. Karpenko, Aircraft hydraulic drive energy losses and operation delay associated with the pipeline and fitting connections, Aviation 28 (2024) 1–8, https://doi.org/10.3846/aviation.2024.20946.
[47] N.M.C. Martins, B. Brunone, S. Meniconi, H.M. Ramos, D.I.C. Covas, CFD and 1D approaches for the unsteady friction analysis of low Reynolds number turbulent flows, J. Hydraul. Eng. 143 (2017) 04017050, https://doi.org/10.1061/(ASCE)HY.1943-7900.0001372.
[48] J. Lee, V.K. Lohani, A.M. Dietrich, Loganathan GV Hydraulic transients in plumbing systems, Water Sci. Technol. Water Supply 12 (2012) 619–629, https://doi.org/10.2166/ws.2012.036.
[49] J. Lee, Hydraulic transients in service lines, Int. J. Hydraul. Eng. 4 (2015) 31–36, https://doi.org/10.5923/j.ijhe.20150402.02.
[50] J. Lee, M. Meehan, Survival analysis of US water service lines utilizing a nationwide failure data set, J. Am. Water Works Assoc. 109 (2017) 13–21.
[51] E.B. Wylie, V.L. Streeter, Fluid transients in systems, Prentice Hall Inc., 1993.
[52] I. Pothof, B. Karney, Guidelines for transient analysis in water transmission and distribution systems, in: A. Ostfeld (Ed.), Water supply system analysis: Selected topics, InTech, 2012, https://doi.org/10.5772/53944.
[53] F. Castellani, C. Capponi, B. Brunone, M. Vedovelli, S. Meniconi, Performance assessment of pneumatic-driven automatic valves to improve pipeline fault detection procedure by fast transient tests, Sensors 1825 (2024) 24, https://doi.org/10.3390/s24061825.
[54] A. Atarodi-Kashani, S. Delfani, M. Khademi, M. Shafaie, Investigation of long-term rupture pressure in PEX-AL-PEX composite pipes, Int. J. Press. Vessels Pip. 200 (2022) 104790, https://doi.org/10.1016/j.ijpvp.2022.104790.
[55] A.A. Oleiwi, H. Afrasiab, A. Zolfaghari, A comprehensive finite element framework for modeling of PEX-Al-PEX composite pipes, Int. J. Press. Vessels Pip. 212 (2024) 105358, https://doi.org/10.1016/j.ijpvp.2024.105358.
[56] M.H. Chaudhry, Applied Hydraulic Transients, 3rd Edition., Springer, 2013.
[57] D. Covas, I. Stoianov, H. Ramos, N. Graham, Maksimovic C the dynamic effect of pipe-wall viscoelasticity in hydraulic transients. Part I – experimental analysis and creep characterization, J. Hydraul. Res. 42 (2003) 517–532, https://doi.org/10.1080/00221686.2004.9641221.
[58] D. Covas, I. Stoianov, J.F. Mano, H. Ramos, N. Graham, C. Maksimovic, The dynamic effect of pipe-wall viscoelasticity in hydraulic transients. Part II – model development, calibration and verification, J. Hydraul. Res. 43 (2003) 56–70, https://doi.org/10.1080/00221680509500111.
[59] A.K. Soares, D.I.C. Covas, L.F.R. Reis, Analysis of PVC pipe-wall viscoelasticity during water hammer, J. Hydraul. Eng. 134 (2008) 1389–1394, https://doi.org/10.1061/(ASCE)0733-9429(2008)134:9(1389).
[60] H.-F. Duan, M.S. Ghidaoui, P.J. Lee, Y.K. Tung, Unsteady friction and viscoelasticity in pipe fluid transients, J. Hydraul. Res. 48 (2010) 354–362, https://doi.org/10.1080/00221681003726247.
[61] S. Meniconi, B. Brunone, M. Ferrante, C. Massari, Transient hydrodynamics of in-line valves in viscoelastic pressurized pipes: long-period analysis, Exp. Fluids 53 (2012) 265–275, https://doi.org/10.1007/s00348-012-1287-3.
[62] G. Pezzinga, B. Brunone, S. Meniconi, Relevance of pipe period on Kelvin-Voigt viscoelastic parameters: 1D and 2D inverse transient analysis, J. Hydraul. Eng. 142 (2016) 04016063, https://doi.org/10.1061/(ASCE)HY.1943-7900.00012.
[63] T. Walski, D.V. Chase, D. Savic, W. Grayman, S. Beckwith, E. Koelle, Advanced water distribution modeling and management, Haestad Press, Waterbury, 2003.
[64] D. Misiunas, Failure monitoring and asset condition assessment in water supply systems, Lund University, 2005. PhD Thesis.
[65] E.J.M. Blokker, J.H.G. Vreeburg, J.C. van Dijk, Simulating residential water demand with a stochastic end-use model, J. Water Res. Plan. Man. 136 (2010) 19–26, https://doi.org/10.1061/(ASCE)WR.1943-5452.0000002.
[66] C. Douglas, S. Buchberger, P. Mayer, Systematic oversizing of service lines and water meters, AWWA Water Sci. 1 (2019) e1165.